J Bone Miner Metab (2013) 31:399–408
DOI 10.1007/s00774-013-0436-y

ORIGINAL ARTICLE

Delayed fracture healing in tetranectin-deficient mice

Kousuke Iba · Yasuhisa Abe · Takako Chikenji · Kumiko Kanaya · Hironori Chiba · Koichi Sasaki · Takayuki Dohke · Takuro Wada · Toshihiko Yamashita

Received: 20 June 2012 / Accepted: 31 January 2013 / Published online: 16 April 2013

Abstract Tetranectin is a plasminogen-binding protein that enhances plasminogen activation, which has been suggested to play a role in tissue remodeling. Recently, we showed that tetranectin has a role in the wound-healing process. In this study, we investigated whether tetranectin plays a role in fracture healing. The fracture-healing process was studied using a femoral osteotomy model in tetranectin-null mice, previously generated by the authors. Radiographic imaging, micro-computed tomography (μCT), and histological analysis were used to evaluate osteotomy healing. In wild-type mice, a callus was apparent from 7 days, and most samples showed marked callus formation and rebridging of the cortices at the osteotomy site at 21 days. In contrast, in the tetranectin-null mice there was no callus formation at 7 days and much less callus formation and no bridging of cortices were observed at 21 days. At 35 days, all osteotomy sites showed clear rebridging, and secondary bone formation was achieved in wild-type mice by 42 days. In contrast, no clear rebridging or secondary bone formation was observed at 42 days in the tetranectin-null mice. Analysis using μCT at 21 days after osteotomy revealed that the callus area in tetranectin-null mice was smaller than that in wild-type mice. Histological analysis also showed that soft tissue and callus formation were smaller in the tetranectin-null mice at the early stage of the healing process after drill-hole injury. These results suggested that tetranectin could have a role in the positive regulation at the early stage of the fracture-healing process, which was reflected in the delayed fracture healing in tetranectin-deficient mice.

Keywords Tetranectin · Fracture healing · Delay · Stage · Knockout mouse

K. Iba (✉) · Y. Abe · K. Kanaya · H. Chiba · K. Sasaki · T. Dohke · T. Wada · T. Yamashita
Department of Orthopaedic Surgery, Sapporo Medical University School of Medicine, South-1, West-16, Chuo-ku, Sapporo 060-8543, Japan
e-mail: iba@sapmed.ac.jp

T. Chikenji
Department of Occupational Therapy, Sapporo Medical University School of Health Science, South-1, West-16, Chuo-ku, Sapporo 060-8543, Japan

Introduction

Fracture healing is a sequential process that has been divided into soft tissue formation, which includes hematoma and fibrous tissue formation, inflammation, angiogenesis, and mesenchymal progenitor recruitment; cartilage and callus formation; and callus remodeling with a series of molecular and cellular events [1]. Remodeling of the callus leads to restoration of the anatomic and biomechanical properties of the original skeletal element [2]. A number of factors have been shown to influence fracture repair, and analyses of the molecular basis for these abnormalities have led to a greater understanding of this process [3–8].

Tetranectin belongs to the family of C-type lectins and is composed of three identical, noncovalently linked 20-kDa subunits [9, 10]. It was originally purified from human serum on the basis of its plasminogen kringle 4-binding properties [11]. Tetranectin is produced by many cell types and is present in serum at a concentration of 10 mg/l [10]. Although the biological function of tetranectin has not yet been clarified, it is known to enhance plasminogen activation by tissue-type plasminogen activators and binds to fibrin, calcium, heparin, and other

sulfated polysaccharides [9–11]. The binding properties of tetranectin could include a role in tissue remodeling. Recently, we showed that the healing of incisional skin wounds was markedly delayed in tetranectin-null mice, indicating that tetranectin could have a function in the cutaneous wound-healing process [12, 13]. Cutaneous wound healing is a dramatic example of a tissue-remodeling process mediated by a large number of growth factors, cytokines, and matrices [14], and is presented as three overlapping series of events: inflammation, new tissue formation, and matrix remodeling [15]. In terms of phases, the process of bone fracture healing, which includes inflammation, callus formation, and remodeling of the callus to mature lamellar bone [16], is similar to cutaneous wound healing. The early process, in particular, of the tissue-remodeling process is the same for cutaneous wounds and fractures, and involves hematoma formation, a matrix rich in fibrin and fibronectin, and the infiltration of neutrophils and macrophage [15, 17]. After these processes, mesenchymal progenitors make up the fibrous tissues and granulation tissue around the defect in the injured fields. Additionally, a previous in vitro study showed that tetranectin is expressed during bone formation [18]. We thus hypothesized that tetranectin might play a significant role in fracture healing.

In this study, we investigated whether tetranectin plays a role in fracture repair using two bone-healing models in tetranectin-null mice: a femoral diaphyseal osteotomy model and a tibial drill-hole model. The former is a suitable model for the investigation of the overall process of fracture healing and the latter model is appropriate for the study of early change of the injured fields [19, 20].

Materials and methods

Experimental animals

The wild-type and tetranectin-null mice (C57/BL/6 J background) used in this study were described previously [12]. The wild-type mice were littermates and served as controls. All animals were maintained in our animal facility under specific pathogen-free conditions, and all animal work was reviewed and approved by the Institutional Animal Care and Use Committee of Sapporo Medical University.

Fracture model

A transverse osteotomy of the femur diaphysis and a tibial drill-hole were generated in 10-week-old wild-type and tetranectin-null mice [12]. Groups of wild-type mice ($n = 78$) and tetranectin-null mice ($n = 76$) were anesthetized with pentobarbital (0.5 ml/kg) for experiments. Six mice from each group were used for radiologic analysis during osteotomy healing, 8 mice for micro-computed tomography (μCT) analysis, 10 mice for histological analysis of the transverse osteotomy model, 11 mice for histological analysis of the drilling model, 22 mice for the primary culture to observe mineralization and colony-forming units (CFUs) in vitro, and 16 mice for RNA isolation from the primary culture. The experiment was unsuccessful in the remaining 5 wild-type and 3 tetranectin-null mice because of failure of femoral diaphyseal osteotomy or the tibial hole-drilling procedure.

Femoral diaphyseal osteotomy model

The left femur was subjected to transverse osteotomy at the femoral midshaft using bone scissors. The displaced osteotomy site was repositioned and stabilized with an intramedullary nail (0.8 mm in diameter) as previously reported [19]. At 7, 14, 21, 28, 35, 42, 49, 56, 63, and 70 days after osteotomy, radiographic images and samples for histological analysis were obtained from at least four mice per data point. Radiographs were taken with a soft X-ray apparatus (CMB-2; Softex, Tokyo, Japan) using industrial X-ray film (IX; Fuji Film, Tokyo, Japan).

Tibial drill-hole model

In addition, drilling of the left tibia as reported previously with modifications [20] was performed to evaluate early changes in the fracture-healing process, including fibrous tissue and granulation tissue formation around the defect in the injured fields. Briefly, a transverse hole was made at a point just below the patella tendon insertion of the tibia using a nail (0.8 mm in diameter), although the original method used a longitudinal drilling of the femur and tibia [20]. The nail was inserted deep into the marrow space to reach the other edge of the cortical bone. The tibias of 8 wild-type and 8 tetranectin-null mice were isolated at 3 days and at 10 days after drilling, and soft tissue and callus formation was evaluated by histological analysis. In addition, the tibias of 3 wild-type and 3 tetranectin-null type mice were isolated at 1 day and 3 days after drilling for analysis of tetranectin expression in the soft tissue of the drill-hole site.

Radiological analysis

Radiographs at 7, 14, 21, 28, 35, 42, 49, 56, 63, 70, and 84 days after osteotomy were independently assessed by two investigators using a scoring scale of 0–7 based on the rebridgement of the cortices and acceleration of healing as described previously [21]. The scoring was as follows: 0, no bridging or callus formation; 1, no bridging, but initiation of a small amount of callus; 2, no bridging, but

obvious callus formation near and around the osteotomy site; 3, no bridging, but marked callus formation near and around the fracture site; 4, rebridging of at least one cortex, and marked callus formation near and around the osteotomy site; 5, rebridging of at least one cortex, and marked and complete callus formation around the osteotomy site; 6, rebridging of both cortices, and/or some resolution of the callus; and 7, clear rebridging of both cortices and resolution of the callus [21]. Scoring was completed and results were expressed as mean scores of at least four samples at each time point after osteotomy.

Micro-computed tomography

Isolated femoral bone samples at 21 days after osteotomy were fixed in 10 % neutral buffered formalin and analyzed using a micro-CT scanner (ScanXmate-L090; Comscantecno, Yokohama, Japan) operated at a lamp voltage of 70 kV and current of 100 μA. The isolated femurs of 8 wild-type and 8 tetranectin-null mice at 21 days after osteotomy were scanned on the micro-CT system using X sys FP Version 1.7 and coneCTexpressIV 1.32 (Comscantecno) operating software. Callus and new bone formation in the osteotomized femurs were investigated. Samples were scanned at a magnification factor of 7.1 and spatial resolution of 14.1 μm/pixel, and captured images were then rendered using software (TRI/3D BON; Ratoc System Engineering, Tokyo, Japan). Quantitative assessment of callus and new bone formation was performed at the central region of each callus. The endocortical surface of the newly formed cortical bone was identified with the contouring function of the analytical software (TRI/3D BON; Ratoc System Engineering), and supplemented manually to measure the total tissue area. The calcified pixels at 14.13 μm/pixel were binarized in the range from 31 to 224 in a grayscale of 0–255. The callus tissue area was measured by subtracting the original bone area, which was measured by contouring the external surface of the femur, from the total tissue area. The newly formed bone in the callus tissue area was calculated by setting the same threshold value for the calcified pixels.

Histological analysis

For the analysis of callus formation and bone healing, each of five femur samples obtained at 21 and 28 days after osteotomy were fixed in 10 % neutral buffered formalin for 14 days, decalcified in 0.5 M ethylenediaminetetraacetic acid (EDTA) for 3 days, and embedded in paraffin. Paraffin sections were cut in the sagittal plane at a thickness of 4 μm. The sections of each femur were stained with hematoxylin and eosin (H&E) and Alcian blue–nuclear fast red. Slide images were captured using a Super Coolscan 5000 ED system (Nikon, Tokyo, Japan). Total area of the external callus and cartilage at the osteotomy site was quantified [22] using ImageJ (NIH). For the analysis of soft tissue formation before callus formation, the tibia samples with transverse holes at 3 and 10 days were prepared in the same manner as the femoral bone and stained with H&E. The average width of the soft tissue at the center of the cortical defect was measured using the samples taken.

Immunohistochemistry

For evaluation of tetranectin distribution, immunohistochemical staining for tetranectin was performed on the tibia samples with transverse holes. At 1 and 3 days after drilling, tibia samples were fixed in 4 % paraformaldehyde for 2 days, decalcified using 0.5 M EDTA for 3 days, and embedded in Tissue-Tek O.C.T. Compound (Sakura Finetek, Torrance, CA, USA), after which longitudinal sections were cut at a thickness of 8 μm. To inactivate the endogenous peroxidase, the sections were treated with 0.1 % H_2O_2 in 0.1 M phosphate-buffered saline (PBS) for 30 min at room temperature (RT). After washing for 10 min with 0.1 M PBS containing 0.3 % Triton X-100 (PBST), the sections were treated with 2 % bovine serum albumin (BSA) at RT for blocking. After further washing for 10 min with 0.1 M PBST, the sections were incubated for 12 h with a primary antibody against tetranectin (Abcam, Cambridge, MA, USA) diluted 1:500 in PBST at 4 °C. After washing for 30 min with 0.1 M PBST, the sections were incubated for 2 h with a secondary antibody (Vector Laboratories, Burlingame, CA, USA) diluted 1:500 in PBST at RT. Sections were then washed for 30 min with PBST and placed for 2 h in an avidin–biotin–peroxidase complex (ABC kit; Vector Laboratories, Burlingame, CA, USA) diluted 1:1,000 in PBST at RT. The immunoreactions were rendered visible by reaction with 0.05 M Tris–HCl buffer (pH 7.6) containing 0.01 % 3,3′-diaminobenzidine (DAB) (Sigma-Aldrich, St. Louis, MO, USA), and 0.0003 % H_2O_2 for 30 min at RT. Finally, slides were counterstained with hematoxylin QS (Vector Laboratories), dehydrated, and mounted on glass slides. The morphology of the positive staining was evaluated with light microscopy.

Cell culture

Bone marrow stromal cells were obtained from the excised femurs of 16 mice without osteotomy experimentation by flushing the shafts with Dulbecco's modified Eagle's medium (DMEM). The cells were cultured in DMEM containing 10 % fetal bovine serum (FBS), 4 mM L-glutamine, and

penicillin (100 U/ml)/streptomycin (100 ng/ml). For induction of osteoblastogenic differentiation, the adherent bone marrow stromal cells were treated with a medium consisting of DMEM supplemented with 10 % FBS, 50 μg/ml ascorbic acid, and 10 mM β-glycerophosphate for 21 days. Mineralization was observed from 14 to 21 days, and the cultures were stained with alizarin red S after culture for 21 days [12].

For measurement of the numbers of fibroblastic CFUs and osteoblastic CFUs, bone marrow stromal cells were seeded by flushing both the femur shafts of a mouse into 35-mm culture dishes (Becton–Dickinson, Franklin Lakes, NJ, USA). At 3 days after seeding, cultured cells were fixed with 4 % paraformaldehyde for 2 days. The cultured cells were stained with 0.2 % methylene blue for fibroblastic CFUs and alkaline phosphatase (ALP) (ALP kit; Muto Pure Chemicals, Tokyo, Japan) for osteoblastic CFUs. The number of methylene blue-positive CFUs and ALP-positive CFUs was counted in four randomly selected fields (10×) per culture dish by light microscopy.

RNA isolation and reverse transcription-PCR (RT-PCR)

RNA was isolated from the bone marrow stromal cell culture using Trizol (Gibco BRL, Gaithersburg, MD, USA) at 7 days after the induction of osteoblastogenic differentiation. Reverse transcriptase-polymerase chain reaction (RT-PCR) was performed as described previously [12, 13]. Conditions applied for PCR were 96 °C for 30 s, 25 or 30 cycles of 96 °C for 15 s, 55 °C for 30 s, 72 °C for 1 min, and 72 °C for 7 min using a Perkin Elmer/Cetus Thermocycler Model 2400. The primers used to detect type I collagen (Col I), osteopontin (OPN), osteocalcin (OC), and glyceraldehyde-3-phosphate dehydrogenase (G3PDH) were as follows: 5′-AATGGTGAGACGTGGA AACCCGAG (forward primer) and 5′-CGACTCCTACATCTTCTGAGTTTGG (reverse primer) for Col I, 5′-GACCATGAGATT GACAGATTTG (forward primer) and 5′-TGATGT TCCAGGCTGCCA GAGTTTG (reverse primer) for OPN, 5′-GACAAAGCCT TCATGT CCAAGC (forward primer) and 5′-AAA GCCGCTGCCAGAGTTTG (reverse primer) for OC, and 5′-ACCACAGTCCATGCCATCA C (forward primer) and 5′-TCCACCACCCTGTTGCTGTA (reverse primer) for G3PDH.

Statistical analyses

Data were expressed as mean ± SD. Statistical analyses were performed using Student's t test. $p < 0.05$ was considered to indicate statistical significance.

Results

Bone healing in tetranectin-null mice

In wild-type mice, a calcified callus was apparent from 7 to 14 days, and most samples showed marked callus formation and rebridging of the cortices of the osteotomy site at 21 days. In contrast, there was no callus formation at 7 days, and much less callus formation over the osteotomy site and little bridging of the cortices were observed at 21 days in tetranectin-null mice. At 35 days, all osteotomy sites showed clear rebridging of both cortices and resolution of the callus, and secondary bone formation and remodeling were achieved in all wild-type mice by 42 days. In contrast, no clear rebridging of both cortices and resolution of the callus was observed at 42 days in tetranectin-null mice, with these steps taking at least 63 days to be completed in the tetranectin-null mice (Fig. 1a). At 70 days, secondary bone formation and remodeling were not

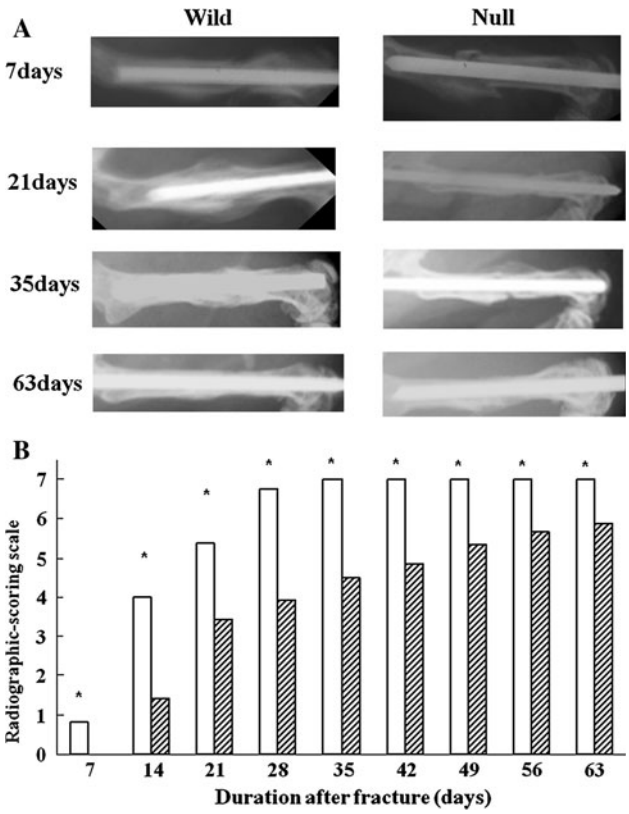

Fig. 1 Radiologic analysis of osteotomy healing in tetranectin-null mice. **a** Radiographic images were evaluated at 7, 21, 35, and 63 days after transverse femoral osteotomy. Osteotomy healing processes in tetranectin-null mice (*Null*) were much delayed compared to those in wild-type mice (*Wild*). **b** A semiquantitative evaluation based on our scoring scale [22] showed that the osteotomy healing process in tetranectin-null mice (*hatched bars*) was significantly delayed compared with that in wild-type mice (*white bars*)

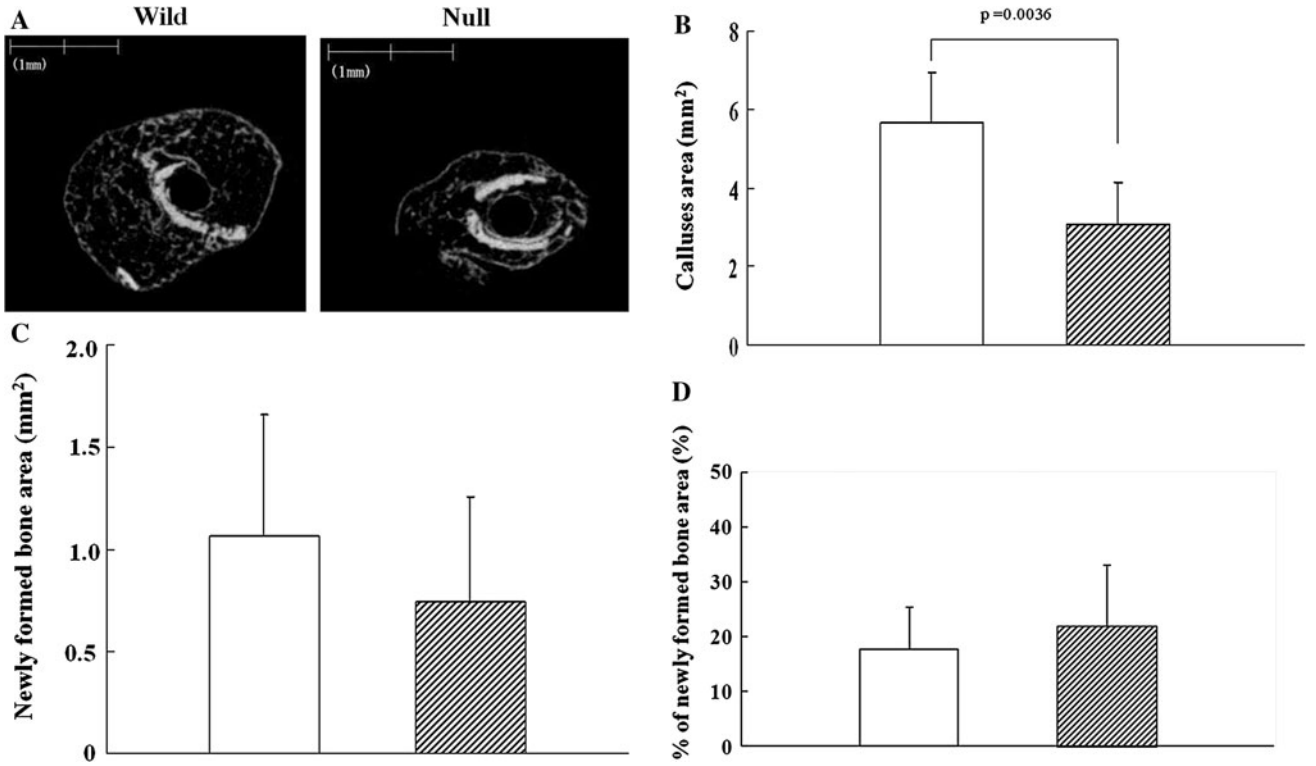

Fig. 2 Micro-computed tomography (μCT) transverse images of callus at 21 days after osteotomy. **a** The callus size in wild-type mice (*Wild*) was greater than that in tetranectin-null mice (*Null*). **b** Quantitative analysis of transverse slides taken from the central region of the callus in each sample showed that the average value of the callus area in wild-type mice (*white bar*) was significantly greater than that in tetranectin-null mice (*hatched bar*). **c** The average area of newly formed bone in the callus in wild-type mice (*white bar*) was greater than that in tetranectin-null mice (*hatched bar*), although the difference was not statistically significant. **d** The ratio of newly formed bone area to callus area (% of new bone area) in the wild-type mice (*white bar*) was not significantly different from that in tetranectin-null mice (*hatched bar*) (**d**)

yet completed in most tetranectin-null mice, taking 84 days for completion in all mice (data not shown). The mean scores based on the scoring scale [21] for wild-type mice at 7, 14, 21, 28, 35, 42, 49, 56, and 63 days after femoral transverse osteotomy were 0.8, 4.0, 5.4, 6.8, 7.0, 7.0, 7.0, 7.0, and 7.0, respectively, whereas those for tetranectin-null mice were 0 ($p = 0.00021$), 1.4 ($p = 0.00015$), 3.4 ($p < 0.0001$), 3.9 ($p < 0.0001$), 4.5 ($p = 0.0032$), 4.9 ($p < 0.0001$), 5.3 ($p = 0.037$), 5.7 ($p = 0.047$), and 5.9 ($p = 0.006$), respectively, which were significantly lower than those of wild-type mice at all measured time points (Fig. 1b).

Micro-computed tomography

Micro-computed tomography (μCT) images revealed that the callus size in wild-type mice was greater than that in the tetranectin-null mice (Fig. 2a). Quantitative analysis of transverse slides taken from the central region of each callus showed that the average value of the callus area in wild-type mice [5.6 ± 1.2 (mean ± SD) mm^2] was significantly greater than that in tetranectin-null mice (3.1 ± 1.0 mm^2) (Fig. 2b). Regarding the newly formed bone in the callus, the average area in the wild-type mice (1.1 ± 0.6 mm^2) was also greater than that in the tetranectin-null mice (0.7 ± 0.5 mm^2), although the difference was not statistically significant (Fig. 2c). On the other hand, there was no significant difference in the ratio of newly formed bone area to callus area (% of new bone area) in the wild-type and tetranectin-null mice (17.7 ± 7.8 and 22.1 ± 10.9 %, respectively) (Fig. 2d).

Histological analysis during bone healing

At 21 days after osteotomy, Alcian blue (Al–B) staining indicated that the cartilage area in the callus was significantly larger in the wild-type mice than that in the tetranectin-null mice (Fig. 3a, b). Histology sections taken at 28 days confirmed a delay in bone healing in the tetranectin-null mice. H&E staining demonstrated that external callus formation was smaller in the tetranectin-null mice than in the wild-type mice (Fig. 3c). Quantitative analysis showed that the average area of external callus formation was significantly smaller (Fig. 3d) and the cartilage area in the callus was significantly larger in tetranectin-null mice than those in the wild-type mice, respectively (Fig. 3e). Regarding the Alcian blue-stained histological sections from the tetranectin-null mice, the cartilage area in the callus at 28 days was increased in comparison with that at

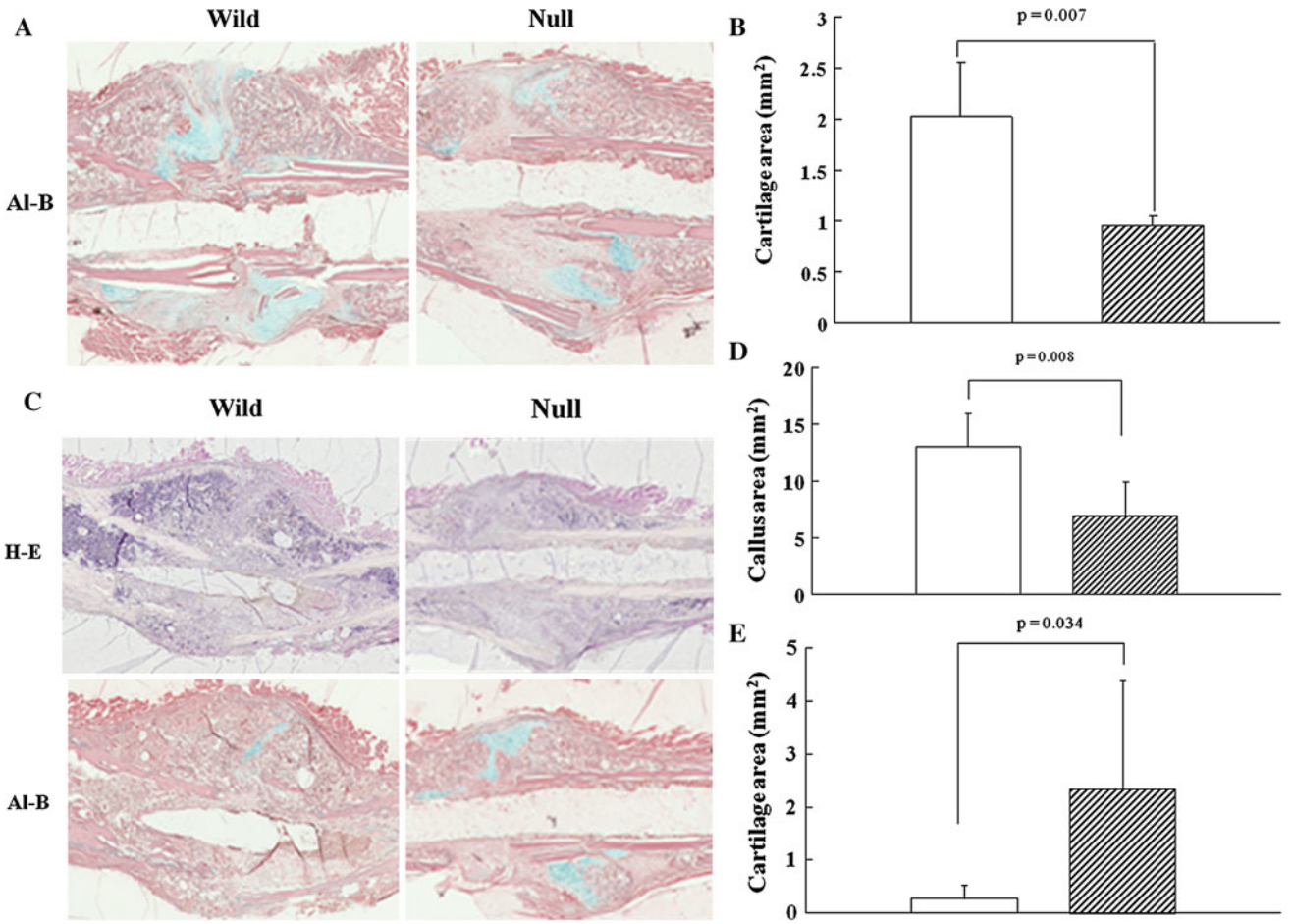

Fig. 3 **a** Histological sections of the osteotomy site at 21 and 28 days. **b** At 21 days after osteotomy, Alcian blue (*Al–B*) staining indicated that the cartilage area in the callus was significantly larger in wild-type mice (Wild, *white bar*) than that in tetranectin-null mice (Null, *hatched bar*). **c** At 28 days, hematoxylin and eosin (*H&E*) staining showed external callus formation was smaller in the tetranectin-null mice than in the wild-type mice. Alcian blue (*Al–B*) staining indicated that cartilage remained in the callus of the tetranectin-null mice. **d** Quantitative analysis showed that the average area of external callus formation was significantly smaller and the cartilage area in the callus was significantly larger in the tetranectin-null mice (*hatched bar*) than in the wild-type mice (*white bar*), respectively (**e**)

21 days (Fig. 3a, b, c, e). At 3 and 10 days after the drilling of the tibia, histological analysis of the cortical defect and bone marrow space revealed that soft tissue (Fig. 4a, day 3), callus, and new bone formation (Fig. 4a, day 10) at the transverse hole were much reduced in the tetranectin-null mice. At 3 days, the average width of the fibrous tissue at the cortical defect in the wild-type mice (0.48 ± 0.08 mm) was significantly thicker than that in the tetranectin-null mice (0.23 ± 0.07 mm, $p = 0.0009$) (Fig. 4b). At 10 days, we could not measure the width of the fibrous tissue because of the callus and new bone formation in wild-type mice (Fig. 4a, day 10).

Immunostaining of tetranectin at the transverse hole of tibia

In wild-type mice, immunohistological analysis showed that there was a considerable amount of tetranectin in the soft tissue at 1 day after drilling (Fig. 5a), and that the level was relatively reduced at 3 days (Fig. 5b). Additionally, fibroblast-like cells were found around those soft tissues (Fig. 5c). In contrast, in tetranectin-null mice, there was no tetranectin around the tibial drill-hole site (Fig. 5d), although fibroblastic cells were observed around those tissues (Fig. 5e).

Differentiation of bone marrow stromal cell culture

No significant differences were observed in the expression of Col I, OPN, or OC, which are osteoblast differentiation markers, between the wild-type and tetranectin-null mice (Fig. 6). In addition, no apparent difference in the degree of mineralization of the cultured cells at 21 days was observed between the wild-type and tetranectin-null mice (data not shown).

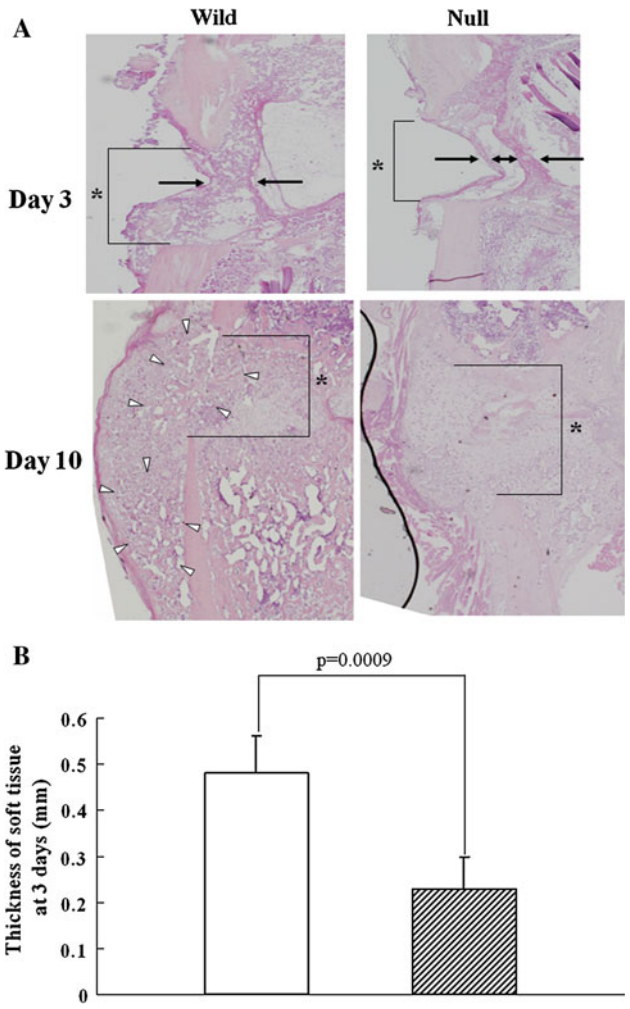

Fig. 4 Early changes in bone healing at tibia hole defects. **a** At 3 days, soft tissue formation (*arrows*) at the cortical defect was much reduced in the tetranectin-null mice tibia (*Null*). At 10 days, callus and newly formed bone (*white arrowheads*) filled the defect in the wild-type mice (*Wild*). In contrast, there was little callus or newly bone formation in the hole defect in the tetranectin-null mice. **b** The average width of the soft tissue at the cortical defect at 3 days in the wild-type mice (*white bar*) was significantly thicker than that in the tetranectin-null mice (*hatched bar*). The width of the lines indicate the drilled hole (*asterisks*), and fibrous tissue thickness is shown as the width between the *arrows*

Regarding the number of methylene blue-positive CFUs (fibroblastic cells) and ALP-positive CFUs (osteoblastic cells) in the bone marrow stromal cell culture, no significant difference was observed between the wild-type and tetranectin-null mice (Fig. 7).

Discussion

We previously generated mice with a targeted disruption in the tetranectin gene (tetranectin-null mice) [12]. Tetranectin-null mice exhibit kyphosis associated with an asymmetrical development of the intervertebral disks, and these findings reveal progressive changes, although the mice appear healthy with no significant changes in bone or other organs. In addition, the mice show no difference in peak bone mineral density (BMD) or changes in BMD following ovariectomy compared with their littermates [12].

The present study showed that soft tissue and subsequent callus formation was delayed in tetranectin-null mice. In contrast, μCT images indicated that the capacity for new bone formation was not influenced by the lack of tetranectin function, and histological analysis showed that the capacity for cartilage formation was maintained and likely to be sufficient for new bone formation in tetranectin-null mice. These results appear to indicate that the capacity for cartilage and new bone formation was maintained even under tetranectin-deficient conditions. Additionally, soft tissue formation at 3 days after hole drilling was much reduced in the tetranectin-null mice.

In the soft tissue at the drill-hole site, tetranectin expression was relatively high at 1 day and reduced at 3 days, and fibroblastic cells were found around those tissues in wild-type mice. In contrast, no tetranectin expression in the soft tissues was observed in tetranectin-null mice, although fibroblastic cells were observed around those tissues.

Therefore, we suggest that the delay in bone healing at the osteotomy and drill-hole sites in tetranectin-null mice might be dependent on the impairment of the early stages of the healing process, such as soft tissue formation.

During the fracture-healing process, mesenchymal progenitors derived from the bone marrow are believed to have an important role in osteoblast differentiation for new bone formation, and defective cell function could be associated with the impairment of fracture healing [23]. In this study, the expression of differentiation markers and mineralization capacity for bone marrow stromal cells in tetranectin-null mice were not significantly different from those in wild-type mice. These findings suggest that bone marrow mesenchymal cells could maintain their capacity to differentiate into osteoblastic cells in tetranectin-null mice. In our previous study, a preosteoblast culture experiment using calvarial osteoblastic cells also indicated that no differences in mineralization capacity existed between wild-type and tetranectin-null mice [12]. Together, these data suggest that the bone formation capacity of mesenchymal progenitor cells in tetranectin-null mice was identical to that in wild-type mice. Recently, it was reported that the bone marrow stromal cell population with in vivo bone formation ability had a significant positive correlation with the expression level of tetranectin [24]. However, that study also found that the gene expression of several other markers was significantly increased in the population, from

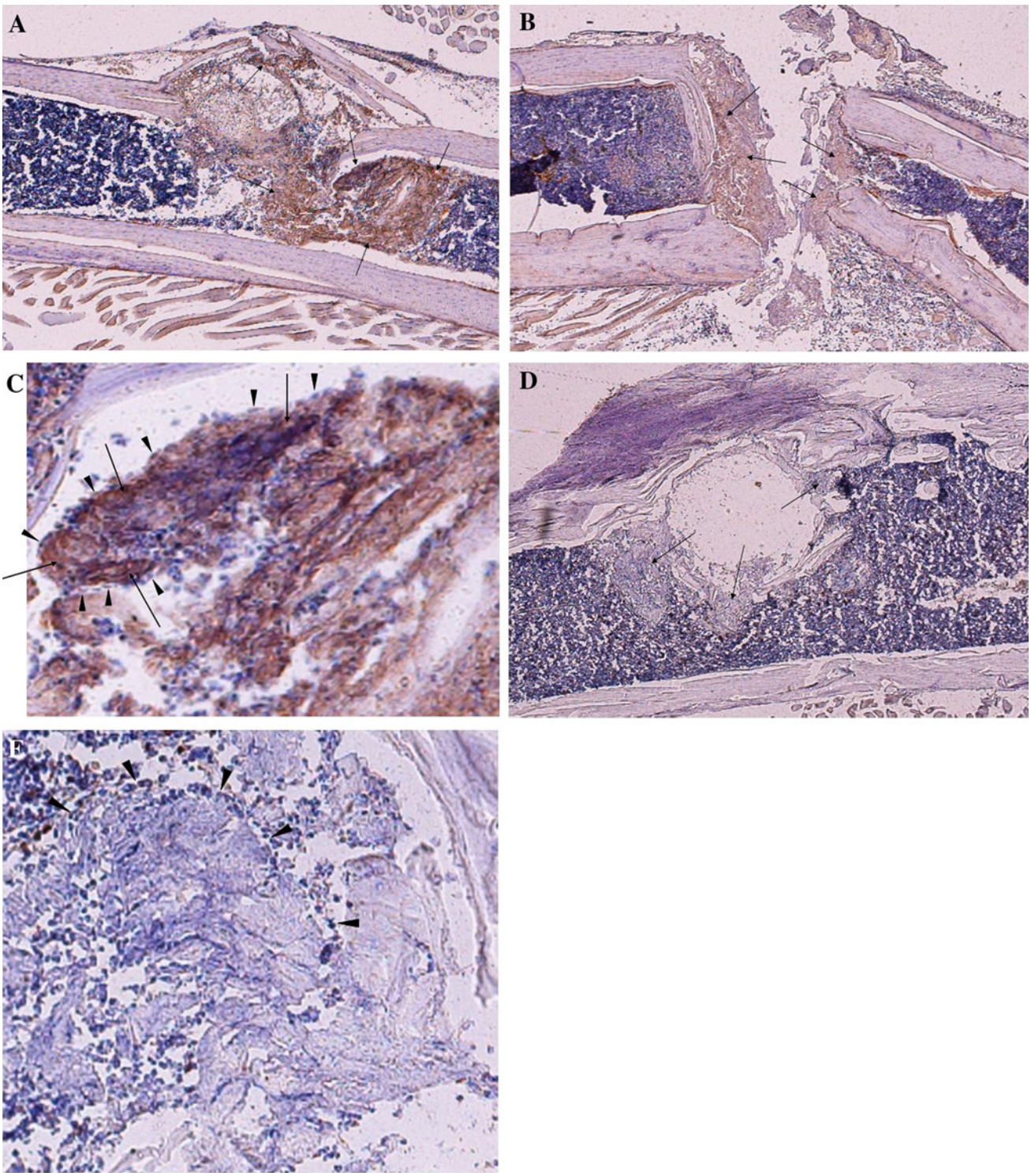

Fig. 5 Tetranectin formation at tibia hole defects. In the wild-type mice, at 1 day, tetranectin was highly expressed in the soft tissue in the hole defect (**a**), and at 3 days, the expression of tetranectin was relatively reduced (**b**). Fibroblastic cells were found around the soft tissue in the wild-type mice (**c**) and in the tetranectin-null mice (**e**; high magnification). In contrast, no tetranectin was expressed in the tetranectin-null mice (**d**). *Arrows* tetranectin expression, *arrowheads* fibroblastic cells

which it could not be concluded that tetranectin regulated the differentiation of bone marrow stromal cells. Additionally, we showed that there was no significant difference in the capacity of bone marrow cells to differentiate into fibroblastic cells based on our experiment using bone marrow cell cultures. Thus, we think that tetranectin could

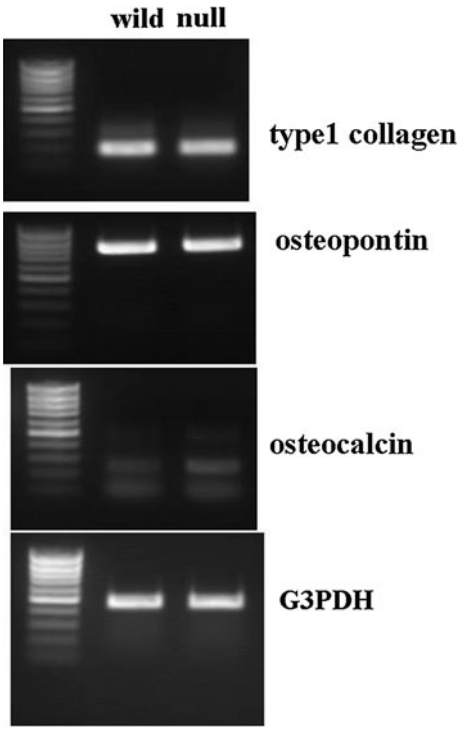

Fig. 6 Expression of differentiation markers in bone marrow cell cultures. At 7 days after the induction of osteoblastogenic differentiation of bone marrow stromal cells, no significant differences were observed in the expression of type I collagen, osteopontin, osteocalcin, or glyceraldehyde-3-phosphate dehydrogenase (G3PDH) between wild-type (*wild*) and tetranectin-null (*null*) mice

have a role in the early stage of the fracture-healing process based on the regulation of soft tissue formation without regulation of mesenchymal progenitor cells.

There were several limitations to this study. First, we did not evaluate the expression levels of molecules associated with the plasminogen system that might be involved in the fracture-healing process. Second, we evaluated μCT data on the basis of two-dimensional analysis and only at 21 days after osteotomy. Third, we did not examine whether tetranectin regulated remodeling of the callus cartilage. Fourth, the surgeons who performed the osteotomy and hole drilling were not blinded to the categorization of the animals into wild-type or tetranectin-null mice, although the analysis of radiographs and μCT were performed blindly.

Overall, 5 to 10 % of all fractures result in impaired healing or nonunion, creating a significant public health problem [25]. From a clinical point of view, the local delivery of therapeutic agents into the lesions would provide an attractive method for the treatment of fractures with impaired healing [26]. Tetranectin is present in human serum, which makes it possible to purify the tetranectin protein [10, 11]. It might be possible to locally deliver purified tetranectin protein from autologous serum to ameliorate impaired fracture lesions, although further study is needed to elucidate the molecular mechanism behind the regulation of soft tissue or callus formation by tetranectin

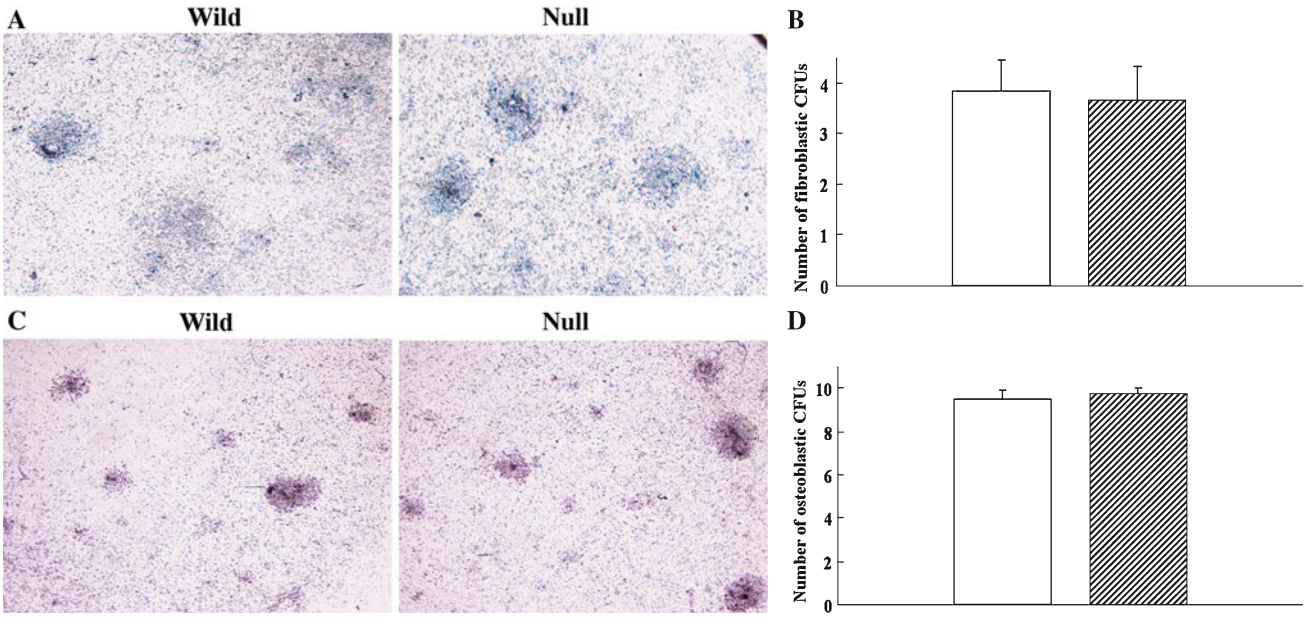

Fig. 7 Formation of methylene blue-positive colony-forming units (CFUs) and alkaline phosphatase (ALP)-positive CFUs in bone marrow cell cultures. Cultured CFUs were stained with methylene blue as the fibroblastic cell marker (**a**) and ALP as the osteoblastic cell marker (**c**). No significant difference was observed in the average number of methylene blue-positive CFUs (**b**) or ALP-positive CFUs (**d**) between the wild-type mice (*white bars*; 3.8 ± 0.63, 9.5 ± 0.43, respectively) and that in the tetranectin-null mice (*hatched bars*; 3.7 ± 0.6, 9.8 ± 0.24, respectively) ($p = 0.659$, 0.588, respectively). The number of CFUs was counted in four randomly selected fields (×10) per culture dish by light microscopy. *Wild* wild-type mice, *Null* tetranectin-null type mice

in the fracture-healing process. We believe that tetranectin might be an attractive candidate as a potential agent to enhance fracture healing.

Acknowledgments The authors thank Mr. Chida and Mr. Murayama (Kureha Special Laboratory Co., Ltd., Iwaki, Japan) for their contributions and advice on μCT analysis. This work was partially supported by grants to K.I. from the Collaboration Center for Community and Industry, Sapporo Medical University.

Conflict of interest The authors report no conflicting interests and have nothing to disclose. The authors alone are responsible for the content and writing of the paper.

References

1. Maes C, Coenegrachts L, Stockmans I, Daci E, Luttun A, Petryk A, Gopalakrishnan R, Moermans K, Smets N, Verfaillie CM, Carmeliet P, Bouillon R, Carmeliet G (2006) Placental growth factor mediates mesenchymal cell development, cartilage turnover, and bone remodeling during fracture repair. J Clin Invest 116:1230–1242
2. Gerstenfeld LC, Cullinane DM, Barnes GL, Graves DT, Einhorn TA (2003) Fracture healing as a post-natal developmental process: molecular, spatial, and temporal aspects of its regulation. J Cell Biochem 88:873–884
3. Colnot C, Thompson Z, Miclau T, Werb Z, Helms JA (2003) Altered fracture repair in the absence of MMP9. Development (Camb) 130:4123–4133
4. Gerstenfeld LC, Cho TJ, Kon T, Aizawa T, Cruceta J, Graves BD, Einhorn TA (2001) Impaired intramembranous bone formation during bone repair in the absence of tumor necrosis factor-alpha signaling. Cells Tissues Organs 169:285–294
5. Shimoaka T, Kamekura S, Chikuda H, Hoshi K, Chung UI, Akune T, Maruyama Z, Komori T, Matsumoto M, Ogawa W, Terauchi Y, Kadowaki T, Nakamura K, Kawaguchi H (2004) Impairment of bone healing by insulin receptor substrate-1 deficiency. J Biol Chem 279:15314–15322
6. Zhang X, Schwarz EM, Young DA, Puzas JE, Rosier RN, O'Keefe RJ (2002) Cyclooxygenase-2 regulates mesenchymal cell differentiation into the osteoblast lineage and is critically involved in bone repair. J Clin Invest 109:1405–1415
7. Kayal RA, Tsatsas D, Bauer MA et al (2007) Diminished bone formation during diabetic fracture healing is related to the premature resorption of cartilage associated with increased osteoclast activity. J Bone Miner Res 22:560–568
8. Gaston MS, Simpson AH (2007) Inhibition of fracture healing. J Bone Joint Surg Br 89:1553–1560
9. Wewer UM, Albrechtsen R (1992) Tetranectin, a plasminogen kringle 4-binding protein, cloning and gene expression pattern in human colon cancer. Lab Invest 67:253–262
10. Høgdall CK (1998) Human tetranectin: methodological and clinical studies. APMIS Suppl 86:7–31
11. Clemmensen I, Petersen LC, Kluft C (1986) Purification and characterization of a novel, oligomeric, plasminogen kringle 4 binding protein from human plasma: tetranectin. Eur J Biochem 156:327–333
12. Iba K, Durkin ME, Johnsen L, Hunziker E, Damgaard-Pedersen K, Zhang H, Engvall E, Albrechtsen R, Wewer UM (2001) Mice with a targeted deletion of the tetranectin gene exhibit a spinal deformity. Mol Cell Biol 21:7817–7825
13. Iba K, Hatakeyama N, Kojima T, Murata M, Matsumura T, Wewer UM, Wada T, Sawada N, Yamashita T (2009) Impaired cutaneous wound healing in mice lacking tetranectin. Wound Rep Regen 7:108–112
14. Martin P, Hopkinson-Wooley J, McCluskey J (1992) Growth factors and cutaneous wound repair. Prog Growth Factor Res 4:25–44
15. Clark RAF (1991) Cutaneous wound repair. In: Goldsmith LA (ed) Physiology, biochemistry, and molecular biology of the skin. Oxford University Press, New York, pp 576–601
16. Einhorn TA (1998) The cell and molecular biology of fracture healing. Clin Orthop Relat Res 355(Suppl):S7–S21
17. Yamaguchi T, Takada Y, Maruyama K, Shimoda K, Arai Y, Nango N, Kosaki N, Tkaishi H, Toyama Y, Matsuo K (2009) Fra-1/AP-1 impairs inflammatory responses and chondrogenesis in fracture healing. J Bone Miner Res 24:2056–2065
18. Wewer UM, Ibaraki K, Schjørring P, Durkin ME, Young MF, Albrechtsen R (1994) A potential role for tetranectin in mineralization during osteogenesis. J Cell Biol 127:1767–1775
19. Doyon AR, Ferries IK, Li J (2010) Glucocorticoid attenuates the anabolic effects of parathyroid hormone on fracture repair. Calcif Tissue Int 87:68–76
20. Tsuji K, Komori T, Noda M (2004) Aged mice require full transcription factor, Runx2/Cbfa1, gene dosage for cancellous bone regeneration after bone marrow ablation. J Bone Miner Res 19:1481–1489
21. Garrett IR, Gutierrez GE, Rossini G, Nyman J, McClukey B, Flores A, Mundy GR (2007) Locally delivered lovastatin nanoparticles enhance fracture healing in rats. J Orthop Res 25:1351–1357
22. Naik AA, Xie C, Zuscik MJ, Kingsley P, Schwarz EM, Awad H, Guldberg R, Drissi H, Puzas JE, Boyce B, Zhang X, O'Keefe RJ (2009) Reduced COX-2 expression in aged mice is associated with impaired fracture healing. J Bone Miner Res 24:251–264
23. Tokunaga A, Oya T, Ishii Y, Motomura H, Nakamura C, Ishizawa S, Fujimori T, Nabeshima Y, Umezawa A, Kanamori M, Kimura T, Sasahara M (2008) RDGF receptor-β is a potent regulator of mesenchymal stromal cell function. J Bone Miner Res 23:1519–1528
24. Larsen KH, Frederiksen CM, Burns JS, Abdallah BM, Kassem M (2010) Identifying a molecular phenotype for bone marrow stromal cells with in vivo bone-forming capacity. J Bone Miner Res 25:796–808
25. Einhorn TA (1995) Enhancement of fracture-healing. J Bone Joint Surg Am 77:940–956
26. Wang W, Nyman JS, Moss HE, Gutierrez G, Mundy GR, Yong X, Elefteriou F (2010) Local low-dose lovastatin delivery improves the bone-healing defect caused by loss of function in osteoblasts. J Bone Miner Res 25:1568–1667